



The Effect of Heat Treatment on Springing of AISI301

Majid Karimian¹, Ehsan Norouzi Isfahani^{2,*}, Mohammad Bagherboom²

1- Mechanical Engineering Department, Khomeinishahr Branch, Islamic Azad University, Khomeinishahr, Esfahan, Iran.

2- Young Researchers and Elite Club, Khomeinishahr Branch, Islamic Azad University, Khomeinishahr, Esfahan, Iran.

*Corresponding Author: ehsan.norouzi@iaukhsh.ac.ir

(Manuscript Received --- 02, 2017; Revised --- 04, 2017; Accepted --- 11, 2017; Online --- 12, 2017)

Abstract

AISI 301 stainless steel is a frequently used metal, especially in high temperature demands and or in part with high corrosion risk. Thin spring steel plates can be used as expansions of heat furnaces insulation and variety of all other springs. The present study has assessed the effects of temperature and thermal treatment time span on the microstructure of stainless steel 301 to achieve elasticity and found out that microstructure gets smaller. As well as the Martensitic α phase in the sample distributes uniformly after thermal treatment at 450 °C for 20 minutes then water quenched in 10 °C. By using X-ray diffraction, it can be found that the reduction in crystalline size of the Martensite α and increasing in Martensite volume fraction is the cause of the elasticity of the samples. All obtained results confirmed by Ferittscope test.

Keywords: Thin spring steel plate, Martensite α , Crystal Grain Size.

1- Introduction

Austenitic stainless steels are the most widely used stainless steel, with excellent corrosion resistance, formability and toughness. These properties make austenitic stainless steels attractive in a range of environments that include chemical, food-processing, high temperature and/or structural loading considerations [1].

In the reinforcement of martensite, the conversion of Austenite to martensite by a shear-free conversion in a steel duct is one of the most commonly used solidification processes. The high strength of Martensite indicates that there are strong dams against

dislocations. Also, Martensite phase can improve fatigue resistance in stainless steels [2].

Therefore, phase transformation becomes an important mechanism for the production of high-performance components. The transformation of the Martensitic phase has been studied by the step-by-step pressurization and the various heat treatments and the achievement of the reinforcement structure.

Due to the cold work, two types of Martensite may be formed in Austenitic stainless steels, α , the crystalline center of cubic crystal network (BCC) and Martensite ϵ , paramagnetic with compact

crystalline hexagonal structure (HCP) [3,4].

The formation of strain-induced Martensite causes changes in mechanical properties and steel corrosion. Two important parameters of M_{d30} and Stacking Fault Energy (SFE) determine the degree of Austenite transformation to Martensite. In fact, M_d is the highest temperature at which a strain-induced martensitic transformation can occur. The parameter M_{d30} is defined as the temperature at which 50% Martensite will form 30% of true strain [4].

In eq. (1), known as the Angel relationship, is one of the most famous relationships with the calculation of the M_{d30} [4].

The formation of Martensite ε and α continuously makes it difficult to understand the mechanism of their formation.

In steady-state Austenite steels during plastic deformation, Austenite transformation to martensitic can occur in a number of ways [4-6].

- 1- $\gamma \rightarrow \varepsilon$
- 2- $\gamma \rightarrow \varepsilon \rightarrow \alpha$
- 3- $\gamma \rightarrow$ Twinning deformation $\rightarrow \alpha$
- 4- $\gamma \rightarrow \alpha$

Typically, the first and second mechanisms are called stress-induced Martensite (SAM) and the third and fourth mechanisms are called strain-induced Martensite (SIM).

The first mechanism is possible only in low strains of up to 10%, and with increasing deformation Martensite α is formed. In the second mechanism of this phase is actually if the range $SFE < 18mj m^{-2}$, Martensite ε is formed as an intermediate phase. In the third mechanism

in higher values $SFE > 18mj m^{-2}$, Twin is present as an intermediate phase. The fourth mechanism is rarely seen and occurs in materials that the high density of dislocations can act as a bud for Martensite α [6].

Over time, several empirical relationships have been proposed for the amount of energy defective generation (SFE). In eq. (2) is presented by Schramn et al. And Rhodes and Thompson (3). Among these relationships, Brofman and Ansell considered the accuracy of the proposed relationship by Schramn weak and seems to be more contributing to Rhodes's relationship [5].

$$M_{d30} = 413 - 462(\%C + \%N) - 9.2\%Si - 8.1\%Mn - 13.7\%Cr - 9.5\%Ni - 18.5Mo \quad (1)$$

$$SFE(mjm^{-2}) = 1.2 + 1.4\%Ni + 0.6\%Cr + 7.7\%Mn - 44.7\%Si \quad (2)$$

$$SFE(mjm^{-2}) = -53 + 6.2\%Ni + 0.7\%Cr + 3.2\%Mn + 9.3\%Mo \quad (3)$$

Lee and Lin explored the morphology of 304L stainless steel. In the samples, Martensite was caused by two types of mechanism, namely, the formation of Martensite due to stress and strain through transmitted electron microscopy. The results showed that the amount of Martensite produced by strain and the rate of hardness and strain rate is directly proportional. It was also concluded that in the strain and the higher strain rate, it can be seen that the Martensite α in the bands has a shear. Fig 1. shows the image of the transmitted electron microscope (TEM) of nucleation martensitic in a sample 304L formed by an impact at the intersection of the shear bond [7].

By looking at the obtained results by Ahmadi and et al, the amount of spring-forward increased by raising the fraction of α -Martensite in V-bent samples [8].

Martensite α in low strains in the form of a layer and with the increase of the strain and the fragmentation of the Martensite blades, its morphology changes to the structure of the dislocation cell, which in the annealing of the nucleus creates high centers of germination and the possibility of reaching the nanostructure / Super fine grain [9].

Using the heat treatment, the properties of these steels are dramatically improved. One type of heat treatment is annealing operation. Heat treatments at a temperature of about 400 °C an increase of Martensite content takes place in Austenitic stainless steels with biphasic structure (Martensite α + Austenite γ) producing an increase of yield stress and ultimate tensile strength [10].

By carrying out annealing in the range of 400-300°C, the amount of Martensite α increases in Austenitic stainless steel. Nucleation sites for the formation of primary alpha Martensite are in areas such as the intersection between the shear bands or between the slip and double bands. Its growth is also due to the frequent emergence of α embryos and its accumulation [11,12].

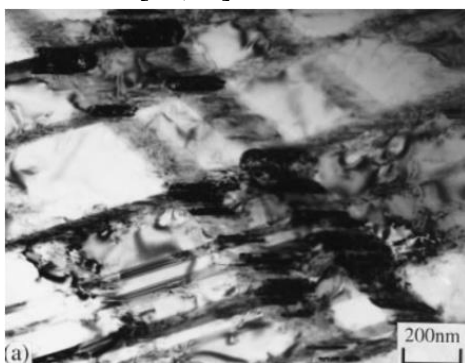


Fig 1. The nucleation of Martensite in deformed specimen image of Martensite at intersection of shear band [7]

There are two different, but consistent, justifications for this phenomenon. Annealing at these temperatures results in recovery mechanisms such as loss of or redesign of point defects, disorientation and defect defects (SFE), which releases the tension around the martensitic layer and thereby its subsequent growth. The second mechanism proposed for this increase in the amount of Martensite is related to the deposition of carbides and the localization of the M_s Temperature, which leads to the formation of more Martensite in the post-annealing. The second justification is more unlikely because the possibility of carbide formation at such a low temperature in Austenitic stainless steel is not present. In addition to the range of 400-300°C, the increase of martensitic α in higher temperatures is also reported [12].

Methods for measuring Martensite content in semi-stable Austenitic stainless steels can be used for magnetic induction (Ferittscope), magnetic equilibrium and magnetometer measurements based on the ferromagnetic phase of Martensite α , X-ray diffraction and density measurement, and Electron Back Scattered Diffraction (EBSD) The basis for the differentiation of crystalline structure and crystalline Austenite, as well as light metallographic photography, is based on the observation of martensitic α , and also using SEM and TEM microscopes and sound emission can also be used as methods for detecting the martensitic phase of α , which is the fastest method commonly used To measure martensitic α , it is used of the Ferittscope [6,13].

In a study by Singh, it shows that during annealing, an hour was cooled on AISI 301 steel, Martensite ϵ up to 200 °C, Martensite α up to 400 °C, and deformation bands in

crystallized areas even Up to 800 °C are stable [14].

The purpose of this study was to investigate the effect of temperature and time of thermal treatment on the Thickness Sheet 301 Thickness and Martensitic Phase α Density by X-Ray Diffraction Pattern as well as Ferittscopic Testing.

2- Materials and methods

In this research, the desired sheet was made of AISI 301 stainless steel with a width of 34 mm and confirmed by the quantum analysis of the accuracy of the steel type. The chemical composition of the steel in question is shown in Table 1. Also in Table 1., the values of SFE and M_{d30} are given according to Rhodes and Angel's relationship. At first, the sheet is cut by flat mold and step press, and a pine punch and matrix are used in order to shape it. Fig 2. shows the sample as a flat. Then these flat parts are created by special molds and adjusting the curve of the desired arch (1.85, 1.35 mm). Finally, in order to create a spring property of 1.85, samples were subjected to annealing at temperatures of 450 and 550 degrees and in an air-cooled furnace, and in order to prevent the deposition of carbides and growth of seeds after annealing over time The corresponding sample was fast quenched in water at 10, 23, and 36 °C.

Table 1- Chemical composition and SFE and M_{d30} of the investigated steel (wt%).

C	Si	Mn	Cr	Mo
0.117	0.55	0.94	17.21	0.194
Ni	Co	Cu	SFE, mJ/m^2	M_{d30} , °C
6.67	0.135	0.298	3.517	43.5

In Fig 3, the image of the sample is considered. It should be noted that the symmetrical shape in the middle of the sample was created for better performance

in the piece that did not play the role of analysis.

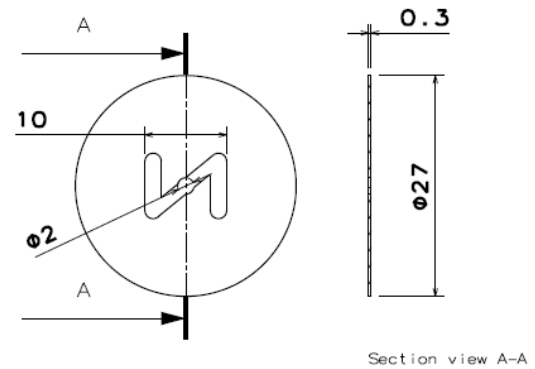


Fig 2. Plate dimensions prior to arcing (nominal sizes in millimeters)

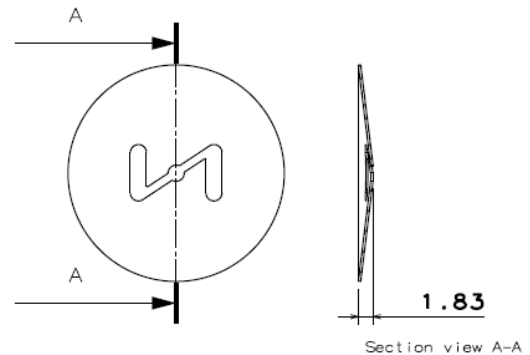


Fig 3. The sample after course press operation (nominal sizes in millimeters)

Images of flat and arched samples in raw form and heat treatment are shown in Fig 4.

3- Results and discussion

The X-ray diffraction (XRD) structural analysis (Phase X-ray diffraction) in a Netherlands-made Phillips model with specifications of 40 kV and 30 mA with a precision of 0.05 degrees per second and a range of 20-100 degrees, The starting angle of the analysis was $2\theta = 30$ and the angle of the end $2\theta=100$. (Wavelength x wavelength copper tube 1.541\AA). Figs. 5-6 analyze the pattern of x-ray diffraction. As seen, the crystalline size of sample 301 prior to the heat treatment of Fig 5. and after the thermal treatment of Fig 6. has changed and one can see the difference

between the samples in terms of peak intensity and crystalline size of the phases, which is calculated according to the XRD results presented in Tables 2-4 and calculated using the Scherrer relation (4). It should be noted that in this connection, K is usually considered to be 0.9 and λ is the wavelength of Cu K α radiation ($\lambda=0.154056$ nm).

$$L = \frac{k\lambda}{\beta \cos \theta} \tag{4}$$

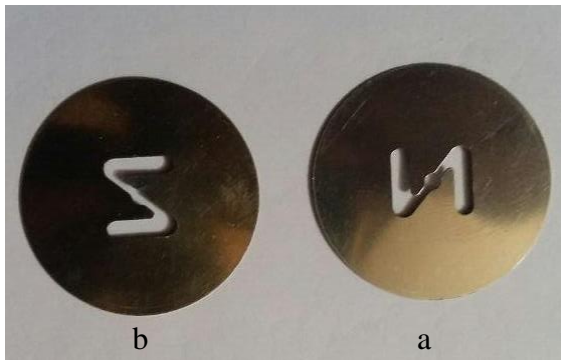


Fig 4. Images of the sample a) before and b) after the heat treatment.

Table 2- Sample peaks prior to thermal operation of Martensite phase \acute{a} .

Peak width according to Radian	Peak intensity	Peak width	Angle 2θ
0.0034	225.15	0.1968	44.5279
0.0069	76.36	0.3936	64.5288
0.012	219.26	0.6888	81.9541

Table 3- Sample peaks undergone thermal operation at 450°C for 20 minutes and cooled in water at 10°C of Martensite phase \acute{a} .

Peak width according to Radian	Peak intensity	Peak width	Angle 2θ
0.006	153.18	0.3444	44.3945
0.0137	98.51	0.7872	64.5652
0.0077	277.55	0.4428	81.9513

The Ferittoscopic test can be used to measure the Martensite \acute{a} . In Table 5., the increase in the martensitic \acute{a} rate is well established and confirms the results of X-ray diffraction. The Ferittscope is a device

used by the magnetic induction method and is commonly used to measure the δ -ferrite phase in Austenitic stainless steel billets, as well as to determine the amount of ferrite phase in Austenite and two-phase stainless steels.

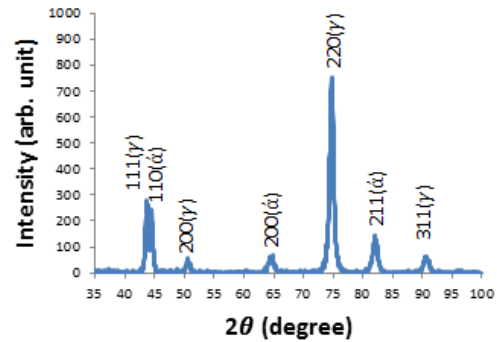


Fig 5. X-ray diffraction patterns of the sample at height 1.85 mm prior to thermal operation

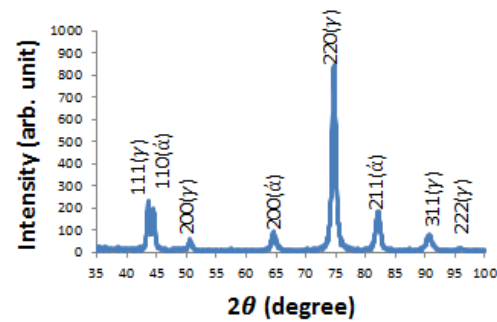


Fig 6. X-ray diffraction patterns of the spring sample at height 1.85 mm undergone thermal operation at 450°C for 20 minutes and cooled in water at 10°C.

It is also used to determine the amount of Martensite in different samples by the magnetic method. This device is portable and has a probe capable of determining the volume fraction of nonmagnetic and magnetic phases of steels by magnetic induction, such that a magnetic field is generated by a coil in a sample and placed on it. Changes in the induced magnetic field, in proportion to the magnitude of the magnetic phase inside the sample, induces a voltage in a secondary winding. By measuring this voltage, we can calculate the volumetric percent of the

magnetization phase. In Table 5, the numbers related to the Ferittoscopic test are related to the volumetric percentage of the magnet phase.

If the phase under research is martensitic phase, to determine the percentage of Martensite in the specimen, the results of the Ferittscope test should be multiplied by 1.7 [6]. It should be noted that the Ferittscopy test was performed with the MP51 model.

Table 4- Mean size of crystals (L) of Austenitic phase and Martensite α (in nanometers) of the sample

	height of sample: 1.85 mm after heating operation (temperature: 450°C time: 20 min quenching: 10°C water)	height of sample: 1.85 mm before heating operation
$L\gamma$	17.3 nm	17.1 nm
$L\alpha$	19.9 nm	27.4 nm

Table 5- Fritscopy test for the sample tested to determine the Martensite α phase in the sample with a precision of ± 0.2

Martenstic volume fraction	Quenched in water (°C)	Annealing temperature (°C)	Time (min)	Height (mm)
13.4	-	-	-	1.35
13.77	-	-	-	1.85
15.81	10	450	20	1.85
16.49	10	450	30	1.85
15.64	10	450	10	1.85
15.55	23	450	10	1.85
15.6	36	450	10	1.85
16.27	36	450	30	1.85
12.47	10	550	30	1.85
14.96	36	550	20	1.85
15.3	23	550	20	1.85
15.4	10	550	20	1.85

4- Conclusion

This study assesses the effects of the thermal treatment on the elasticity of the AISI301 stainless steel. For this purpose, the initial sheet was prepared and then the required shape was formed, finally, under different heat treatments and times, the achieved results are as follow:

1. According to Mangonon et al.'s theory concerning the impact of Austenite stainless steel on the increase of martensitic α at 300-400°C, the crystalline size of the martensitic α increases in the tested sample (AISI301) and thus annealing samples at 450°C results in the elasticity of the samples.
2. The results of the Ferittscopy test and the X-ray diffraction pattern confirmed each other.
3. Due to the Rhodes relationship and the amount of Stacking Fault Energy in the martensitic transformation sample, is the dominant mechanism of deformation.
4. According to the numbers of the Ferittscopy test, height had a direct effect on the amount of the Martensite α , and Martensite increased as the altitude increased.
5. According to the theory of Mangonon, the percentage of Martensite α increased with respect to heat treatment, which in the specimen with a height of 1.85 create springing in the sample.
6. Even though the sample with thermal treatment of 550°C reached the springy, but the degree of reversibility in the sample with thermal treatment of 450°C has a better quality and spring effect, due to the higher percentage of martensitic mercury.
- 7- With fixed annealing temperature at 450°C and water quenching at 10°C, the increase in annealing time causes the increase in Martensite volume fraction.

List of symbols

Peak width at half maximum height (rad)	β
The average crystal size (nm)	L
Crystal form factor	K
Diffraction angle (degree)	θ
X-ray producing tube wavelength(nm)	λ
Crystal Network Cubic Center	α'
Martensite with a Hexagonal Crystal Structure	ε
Austenite	γ

Acknowledgements

The authors wish to express their gratitude for the sponsorship of Young Researchers and Elite Club. Special thanks also go to Dr. Karamian and Mr. Pirestany and Mr. Parastegary, and all those who aided the success of this project.

References

- [1] S.K Paul, N. Stanford, and T. Hilditch, "Austenite plasticity mechanisms and their behavior during cyclic loading," *International Journal of Fatigue.*, vol. 106, pp. 185-195, Jan 2018.
- [2] W. Zeng, and H. Yuan, "Mechanical behavior and fatigue performance of austenitic stainless steel under consideration of martensitic phase transformation," *Materials Science and Engineering.*, vol. 679, pp. 249-257, Jan 2017.
- [3] S. Pirestany, A. Karmanpur, and A. Najafzadeh, "Effect of Operating Conditions on the Formation of Martensite Induced by Rolling Deformation and Resulted Morphology in 201 Austenitic Stainless Steel" Conference, Steel Symposium 93, Yazd, Ardakan Mineral and Industrial Company, Iran, vol. 1, Feb 2015.[in persian]
- [4] P.M. Ahmedabadi, V. Kain, and A. Agrawal, "Modelling kinetics of strain-induced martensite transformation during plastic deformation of austenitic stainless steel," *Materials & Design.*, vol. 109, pp. 466-475, Nov 2016.
- [5] K.H. Lo, C.H. Shek, and J.K.L. Lai, "Recent developments in stainless steels," *Materials Science and Engineering: R: Reports.*, vol. 65, pp. 39-104, May 2009.
- [6] S. Pirestany, "Investigating the effect of strain-induced martensite morphology on formation of nano/ultra fine grained structure in 201 austenitic stainless steel through martensite themomechanical process," Isfahan University of Technology., Msc degree thesis, 2014.[in persian]
- [7] W.S. Lee, and C.F. Lin, "The morphologies and characteristics of impact-induced martensite in 304L stainless steel," *Scripta materialia.*, vol. 43, pp. 777-782, Sep 2000.
- [8] M. Ahmadi, B.M. Sadeghi, and H. Arabi, "Experimental and numerical investigation of V-bent anisotropic 304L SS sheet with spring-forward considering deformation-induced martensitic transformation," *Materials & Design.*, vol. 123, pp. 211-222, June 2017.
- [9] S. Pirestany, A. Karmanpur, and A. Najafzadeh, "Effect of Martensite Induced by Strain Morphology on Microstructure Changes During Back Annealing after Thermo Mechanical Treatment of Martensite in 201 Austenitic stainless steel," Conference, Steel Symposium 94, Kish International Convention Center, Kish, Iran, vol. 1, Feb 2016.[in persian]
- [10] F. Gauzzi, R. Montanari, G. Principi, and M.E. Tata, "AISI 304 steel: anomalous evolution of martensitic phase following heat treatments at 400 °C" *Materials*

Science and Engineering: A., vol. 438-440, pp. 202-206, Nov 2006.

[11] P.L. Mangonon, and G. Thomas, "Structure and properties of thermal-mechanically treated 304 stainless steel," *Metallurgical Transactions.*, vol. 1, pp. 1587-1594, June 1970.

[12] S. Bajda, W. Ratuszek, M. Krzyzanowski, and D. Retraint, "Inhomogeneity of plastic deformation in austenitic stainless steel after surface mechanical attrition treatment," *Surface and Coatings Technology.*, vol. 329, pp. 202-211, Nov 2017.

[13] R. Naraghi, "Martensitic Transformation in Austenitic Stainless Steels," Msc degree thesis, 2009.

[14] J. Singh, "Influence of deformation on the transformation of austenitic stainless steels," *Journal of Materials Science.*, vol. 20, pp. 3157-3166, Sep 1985.